NANO LETTERS

Letter

pubs.acs.org/NanoLett

Synthetic Ligand-Coated Magnetic Nanoparticles for Microfluidic Bacterial Separation from Blood

Jung-Jae Lee,[§,†,‡] Kyung Jae Jeong,[§,†,‡] Michinao Hashimoto,[§,†] Albert H. Kwon,[§,∥] Alina Rwei,[§,†] Sahadev A. Shankarappa,[§,†] Jonathan H. Tsui,[§,†] and Daniel S. Kohane[§,†,*]

[§]Laboratory for Biomaterials and Drug Delivery, Department of Anesthesiology, Division of Critical Care Medicine, Boston Children's Hospital, Harvard Medical School, Boston, Massachusetts 02115, United States

[†]David H. Koch Institute for Integrative Cancer Research, Massachusetts Institute of Technology (MIT), Cambridge, Massachusetts 02139, United States

[∥]Harvard—Massachusetts Institute of Technology Division of Health Sciences and Technology, Cambridge, Massachusetts 02139, United States

Supporting Information

ABSTRACT: Bacterial sepsis is a serious clinical condition that can lead to multiple organ dysfunction and death despite timely treatment with antibiotics and fluid resuscitation. We have developed an approach to clearing bacteria and endotoxin from the bloodstream, using magnetic nanoparticles (MNPs) modified with *bis*-Zn-DPA, a synthetic ligand that binds to both Gram-positive and Gram-negative bacteria. Magnetic microfluidic devices were used to remove MNPs bound to *Escherichia coli*, a Gram-negative bacterium commonly implicated in bacterial sepsis, from bovine whole blood at flows as high as 60 mL/h, resulting in almost 100% clearance. Such devices could be adapted to clear bacteria from septicemic patients.

KEYWORDS: *Sepsis, Zn−DPA, magnetic nanoparticle, microfluidics, bacteria, magnetophoresis*

Bacteremia, the presence of bacteria in the bloodstream, often results in sepsis, which can cause multisystem organ failure[1] and has a high mortality rate of 28−50%.[2] In recent years, the United States has witnessed a sharp increase in the number of sepsis cases due to an aging population, increased use of invasive procedures, and immunosuppressive therapies including cancer chemotherapy and organ transplantation. Consequently, sepsis has become the 11th leading cause of death and seventh leading cause of infant mortality, costing $ 15 billion in treatment in the United States annually.[3,4] The most common treatments for sepsis and septic shock are antibiotics, fluid resuscitation, and vasoactive medications. Additionally, extracorporeal removal of inflammatory mediators,[5] corticosteroids,[6] and recombinant protein drug therapies (e.g., recombinant human activated protein C (Xigris (R))[7] have been introduced as experimental adjunct treatments.[8,9] However, the outcomes have been disappointing, in part because of complications arising from the nonspecific natures of the treatments, resulting in severe bleeding and depletion of modulators of inflammation.[10−15]

Recently, alternative approaches have been sought to address these shortcomings. In particular, antibody-based methods of separating bacteria from blood have been developed for this purpose.[16,17] Here, we have developed magnetic nanoparticles (MNPs) modified with a synthetic ligand, zinc-coordinated bis(dipicolylamine) (***bis*-Zn-DPA**), that can be utilized for highly selective and rapid separation of bacteria and potentially their endotoxins from whole blood using a magnetic microfluidic device. One principal motivation for the use of these ligands is that ***bis*-Zn-DPA** forms coordination bonds with anionic phospholipids which are present at high density on the outer membrane of Gram-positive and Gram-negative bacterial cells, with high selectivity and rapid binding kinetics, as has been demonstrated for optical imaging in murine models.[18−24] The ***bis*-Zn-DPA** coordination complex with specific lipids provides negligible affinity toward normal mammalian cells including white blood cells, or negatively charged proteins such as albumin.[20,25] The faster kinetics of the association of these ligands with bacteria compared to antibody-based approaches could shorten the incubation times required prior to separation[18]—which could facilitate clinical application (e.g., with extracorporeal techniques). Furthermore, these synthetic ligands' ease of synthesis and conjugation to particles present advantages over biomacromolecular ligands that have been used in this context.[16,17,26] They do not suffer the difficulties encountered with biomacromolecular ligands, such as denaturation of the three-dimensional structure and random molecular orientation during covalent immobilization to particles, which can decrease the bioactivity of antibodies by up to 1000 fold.[27] Moreover, antibodies are costly and potentially immunogenic.[28,29] The use of nanoscale magnetic nanoparticles (vs the micrometer-scale particles used in some other magnetophoretic approaches[26]) should enhance ligand loading capacity and mobility in solution, and accelerate the binding kinetics between the particles and bacteria.[30,31] Microfluidic technology was used because of its applicability to the separation and sorting of cells under continuous flow.[16,17,26,32−40] *Escherichia coli* was used as a representative Gram-negative bacterium. The

Received: December 21, 2012
Revised: January 14, 2013

   dx.doi.org/10.1021/nl3047305 | *Nano Lett.* XXXX, XXX, XXX−XXX

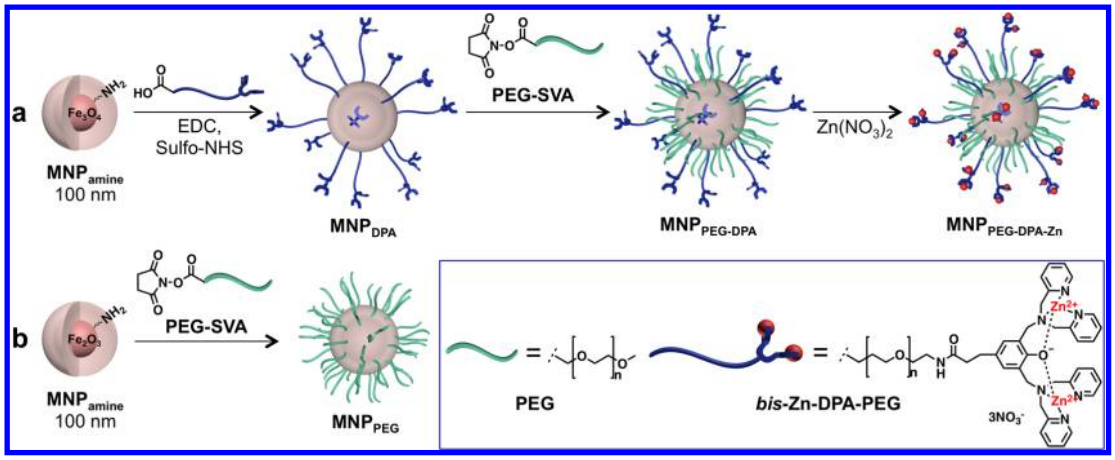

Figure 1. Schema of formation of $\mathbf{MNP_{PEG\text{-}DPA\text{-}Zn}}$ and $\mathbf{MNP_{PEG}}$. (a) $\mathbf{MNP_{amine}}$ was conjugated to ***bis*-DPA-PEG-COOH** *via* carbodiimide chemistry and passivated by **PEG-SVA** (2.0 kDa). Then, Zn^{2+} was coordinated on the DPA to form $\mathbf{MNP_{PEG\text{-}DPA\text{-}Zn}}$ which is capable of targeting bacteria. (b) $\mathbf{MNP_{PEG}}$ was prepared with **PEG-SVA** (2.0 kDa) without the target ligand, ***bis*-Zn-DPA**.

system developed here achieves near complete removal of bacteria at a higher flow rate than with previously reported methods,[16,17,26] and it has the potential to be translated into a treatment for sepsis.

***Bis*-DPA** with a polyethylene glycol (PEG, MW = 10 kDa) spacer (Supporting Information, Figures S1−S4) was immobilized on the surface of amine-terminated MNPs ($\mathbf{MNP_{amine}}$; commercially available aminated Fe_3O_4 nanoparticles, 100 nm in diameter) through carbodiimide chemistry (Figure 1). Unreacted amines on the MNP were passivated by the addition of excess PEG-succinimidyl valerate (**PEG-SVA**, 2.0 kDa) to prevent nonspecific binding from positively charged ammonium ions from unreacted amines at neutral pH. After removing excess **PEG-SVA**, Zn^{2+} was coordinated to the ***bis*-DPA** to create ***bis*-Zn-DPA-PEG-MNP** ($\mathbf{MNP_{PEG\text{-}DPA\text{-}Zn}}$, Figure 1a). MNPs coated only with PEG ($\mathbf{MNP_{PEG}}$) were prepared in the same manner without the addition of the ***bis*-DPA-PEG** (Figure 1b). Carbodiimide chemistry on $\mathbf{MNP_{amine}}$ was validated by a significant decrease in ζ potential upon addition of **PEG-SVA** (from 39 mV to 12 mV, $N = 4$, $p < 0.01$) (Supporting Information, Table S1). When excess **PEG-SVA** was added to ***bis*-DPA**-modified MNPs to remove unreacted amines, the ζ potential decreased from 36 mV to 32 mV ($N = 4$, $p < 0.01$). Furthermore, the chelation of Zn^{2+} with ***bis*-DPA** was evident in the overlapping signals of Fe (from the MNPs themselves) and Zn on the energy dispersive spectra (EDS) from freeze-dried $\mathbf{MNP_{PEG\text{-}DPA\text{-}Zn}}$ (Supporting Information, Figures S5−S7). Only trace amounts of Zn were detected on $\mathbf{MNP_{PEG}}$ or $\mathbf{MNP_{amine}}$ under the same conditions. These results confirmed that both ***bis*-Zn-DPA-PEG** and PEG were successfully immobilized on the surface of MNPs.

The ability of $\mathbf{MNP_{PEG\text{-}DPA\text{-}Zn}}$ to bind to *E. coli* (Figure 2) was demonstrated by mixing green fluorescence-labeled (SYTO 9) *E. coli* (1.0×10^7 CFU/mL) and MNPs (1.0×10^{11}/mL) in PBS for 5 min at room temperature then transferring the mixture to a cell counting chamber slide for visualization by optical microscopy. This concentration of bacteria was selected based on the reported peak blood concentration of *E. coli* after injection of a lethal dose (LD_{100}) *in vivo*.[41] An external permanent magnet was applied to the chamber and dragged across its bottom surface, causing clusters of $\mathbf{MNP_{PEG\text{-}DPA\text{-}Zn}}$ colocalized with *E. coli* to migrate up to several centimeters; co-localization was evidenced by the overlap of phase contrast

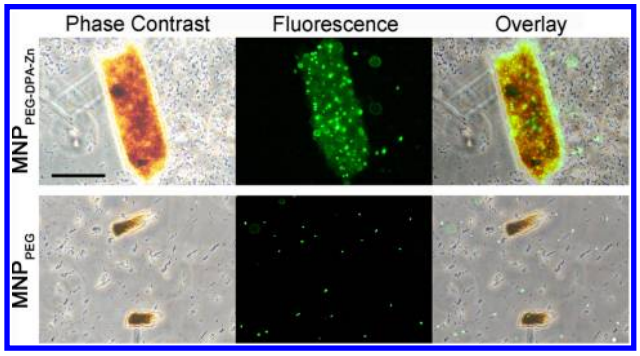

Figure 2. Co-localization of $\mathbf{MNP_{PEG\text{-}DPA\text{-}Zn}}$ with *E. coli*. Clusters of MNPs are visualized in phase contrast (dark brown - MNPs) and prelabeled *E. coli* in green fluorescence. In the presence of a magnetic field (all frames) *E. coli* colocalized with $\mathbf{MNP_{PEG\text{-}DPA\text{-}Zn}}$ (upper panels) but not (b) $\mathbf{MNP_{PEG}}$ (lower panels) Scale bar denotes 100 μm for all images.

images of $\mathbf{MNP_{PEG\text{-}DPA\text{-}Zn}}$ and green fluorescent images of *E. coli* (Figure 2a), clearly indicating binding of $\mathbf{MNP_{PEG\text{-}DPA\text{-}Zn}}$ to *E. coli*. Under the same conditions, no co-localization of *E. coli* and $\mathbf{MNP_{PEG}}$ was observed (Figure 2b), which suggests (1) no interaction between the PEG chains and the bacteria and (2) complete passivation of amine groups on MNPs. The specificity of the binding between ***bis*-Zn-DPA** and *E. coli* was further demonstrated by adding fluorescein (FITC)-labeled ***bis*-Zn-DPA-PEG** molecules to unlabeled *E. coli* (Supporting Information, Figures S8 and S9). Fluorescence microscopy showed that most of *E. coli* were stained with green fluorescence. Minimal fluorescence was detected when FITC-labeled ***bis*-DPA-PEG** (without Zn^{2+}) was added to *E. coli*. FITC-labeled PEG and FITC-labeled amine molecules did not stain *E. coli* effectively regardless of the addition of Zn.

The efficiency of separation of a fixed concentration of *E. coli* (1.0×10^7 CFU/mL) by magnetic separation was measured in PBS with varying concentrations of $\mathbf{MNP_{PEG\text{-}DPA\text{-}Zn}}$ and $\mathbf{MNP_{PEG}}$ (up to 1.0×10^{11}/mL) (Figure 3). After 5 min of incubation in a 1.5 mL test tube, the magnetic field was applied to one side of the tube for 2 min, then the supernatant was collected for quantitation of fluorescent bacteria (see Methods). Enumeration of bacteria using fluorescent labeling and microscopic analysis is a facile and reliable alternative to the standard colony counting method.[42−44] (We confirmed a linear

dx.doi.org/10.1021/nl3047305 | *Nano Lett.* XXXX, XXX, XXX−XXX

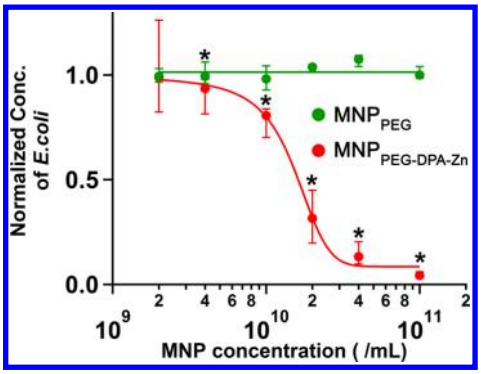

Figure 3. Effect of MNP concentration on separation of *E. coli* (1.0×10^7 CFU/mL) from PBS. *E. coli* concentrations were normalized to the *E. coli* concentration prior to separation. The data were fitted with a sigmoid curve and a straight line with a zero slope for $\mathbf{MNP_{PEG\text{-}DPA\text{-}Zn}}$ and $\mathbf{MNP_{PEG}}$, respectively. Data are medians with 25th and 75th percentiles ($N = 4$). *$p < 0.05$ compared to the initial concentrations.

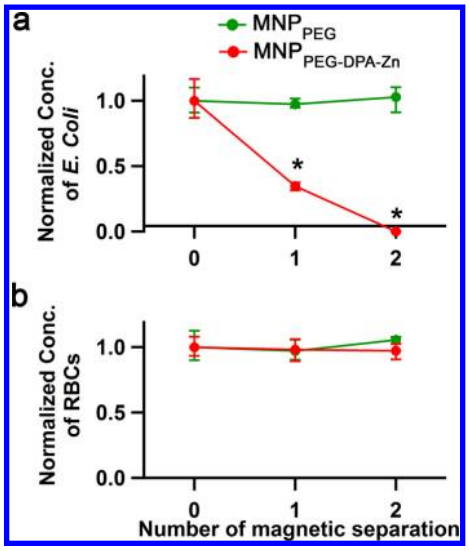

Figure 4. Effect of repeated cycles of magnetic separation on the concentrations in diluted blood of (a) *E. coli* and (b) RBCs. With $\mathbf{MNP_{PEG\text{-}DPA\text{-}Zn}}$, all *E. coli* were removed within two cycles of separation while $\mathbf{MNP_{PEG}}$ did not affect the *E. coli* concentration. The concentration of RBCs was not changed with $\mathbf{MNP_{PEG\text{-}DPA\text{-}Zn}}$ or $\mathbf{MNP_{PEG}}$. *E. coli* and RBC concentrations were normalized to their concentrations prior to separation. Data are medians with 25th and 75th percentiles ($N = 4$). *$p < 0.05$ compared to the initial concentrations. (*E. coli* = 1.0×10^7 CFU/mL, RBC = 1.0×10^8/mL).

correlation between the fluorescent counting method and the colony counting method for *E. coli*; see Supporting Information, Figures S10 and S11). As shown in Figure 3b, 1.4×10^{10} /mL of $\mathbf{MNP_{PEG\text{-}DPA\text{-}Zn}}$ removed 50% of *E. coli* and 1.0×10^{11}/mL of $\mathbf{MNP_{PEG\text{-}DPA\text{-}Zn}}$ completely cleared *E. coli*. In contrast, $\mathbf{MNP_{PEG}}$ did not remove *E. coli* even at the highest MNP concentration. The incubation time required for binding of $\mathbf{MNP_{PEG\text{-}DPA\text{-}Zn}}$ to *E. coli* (<1 min) is significantly shorter than those previously reported for antibody-based bacteria filtration methods (>30 min).[17,26] The accelerated binding rate was perhaps attributable to the high mobility and surface area/volume ratio of magnetic nanoparticles, and the presence of PEG spacers which enhanced the molecular mobility of the ***bis*-Zn-DPA** ligands.

While bacteremia is an important component of the pathogenesis of sepsis, the release of endotoxin from bacteria is a major causative factor in septic shock.[45] Since ***bis*-Zn-DPA** is capable of selective association with endotoxin,[24] we hypothesized that $\mathbf{MNP_{PEG\text{-}DPA\text{-}Zn}}$ could remove endotoxins through magnetic separation. Magnetic separation in a test tube (Supporting Information, Figure S12) decreased the starting concentration of free endotoxin (1.0 EU/mL) in PBS as the concentration of $\mathbf{MNP_{PEG\text{-}DPA\text{-}Zn}}$ increased, to as low as to 9.0% of the starting concentration. $\mathbf{MNP_{PEG}}$ did not affect the free endotoxin concentration. These experiments demonstrate that $\mathbf{MNP_{PEG\text{-}DPA\text{-}Zn}}$ can separate both Gram-negative bacteria and endotoxins from media through magnetophoresis.

The feasibility of using $\mathbf{MNP_{PEG\text{-}DPA\text{-}Zn}}$ to remove bacteria from blood was tested in bovine blood diluted to a red blood cell (RBC) concentration of 1.0×10^8/mL. This concentration, approximately 50 times lower than that of adult human blood ($\sim 5.0 \times 10^9$/mL), was used since higher RBC concentrations obstructed microscopic imaging after magnetic separation. Changes in the RBC concentrations before and after magnetic separation would serve as indicators of the degree of nonspecific binding between MNPs and RBCs. In experiments analogous to those in Figure 3, but using diluted blood instead of PBS, about 70% of *E. coli* were removed during a first cycle (Figure 4a, red circle) of magnetic separation performed on a mixture of RBC, *E. coli* and $\mathbf{MNP_{PEG\text{-}DPA\text{-}Zn}}$ (1.0×10^8/mL, 1.0×10^7 CFU/mL, and 1.0×10^{11}/mL, respectively), a 30% decrease compared to the same process in the absence of blood (Figure 3). A second round of magnetic separation on the same bacterial/blood sample with fresh $\mathbf{MNP_{PEG\text{-}DPA\text{-}Zn}}$ resulted in complete removal of *E. coli* (Figure 4a). The number of RBCs did not change during these experiments, indicating negligible nonspecific interaction with $\mathbf{MNP_{PEG\text{-}DPA\text{-}Zn}}$ (Figure 4b). $\mathbf{MNP_{PEG}}$ did not alter the numbers of *E. coli* or RBCs even after two rounds of magnetic separation (Figure 4a,b). A hemolysis assay confirmed that minimal damage was done to RBCs by $\mathbf{MNP_{PEG\text{-}DPA\text{-}Zn}}$ or $\mathbf{MNP_{PEG}}$ (Supporting Information, Tables S2, S3). These results demonstrate that $\mathbf{MNP_{PEG\text{-}DPA\text{-}Zn}}$ can be used to remove bacteria from blood with minimal nonspecific interaction with RBCs.

A simple microfluidic system (1,000 μm width x 200 μm height) was designed as a proof-of-concept for the removal of *E. coli* from a diluted RBC solution using $\mathbf{MNP_{PEG\text{-}DPA\text{-}Zn}}$. A dual inlet microfluidic system allowed easy separation of MNPs using two laminar flows in a single channel (Supporting Information, Figure S12a). Using this system, we were able to achieve approximately 25% clearance of *E. coli* (Supporting Information, Figures S12b–f and S13; movies S1–S5). However, this system presented difficulties in maintaining two symmetric laminar flows when using whole blood, where there was a large difference with the viscosity of saline (viscosity =1 cP for saline, 10 cP for blood). Although more *E. coli* were still found to be associated with $\mathbf{MNP_{PEG\text{-}DPA\text{-}Zn}}$ than with $\mathbf{MNP_{PEG}}$ at outlet C when using whole blood, many RBCs, *E. coli* and MNPs exited through outlet C even in the absence of a magnetic field.

To address this problem, we created a single-inlet, dual-outlet microfluidic system with three permanent magnets placed in series along the channel (Figure 5a). Bacterial separation from blood was effected by the accumulation of MNPs at the channel walls adjacent to the magnets, instead of by removal through one of the two outlets. $\mathbf{MNP_{PEG\text{-}DPA\text{-}Zn}}$ formed accumulations that contained *E. coli*, whereas $\mathbf{MNP_{PEG}}$ formed clusters without *E. coli* (Figure 5b). Blood containing *E. coli* ($5.0 \times$

dx.doi.org/10.1021/nl3047305 | *Nano Lett.* XXXX, XXX, XXX−XXX

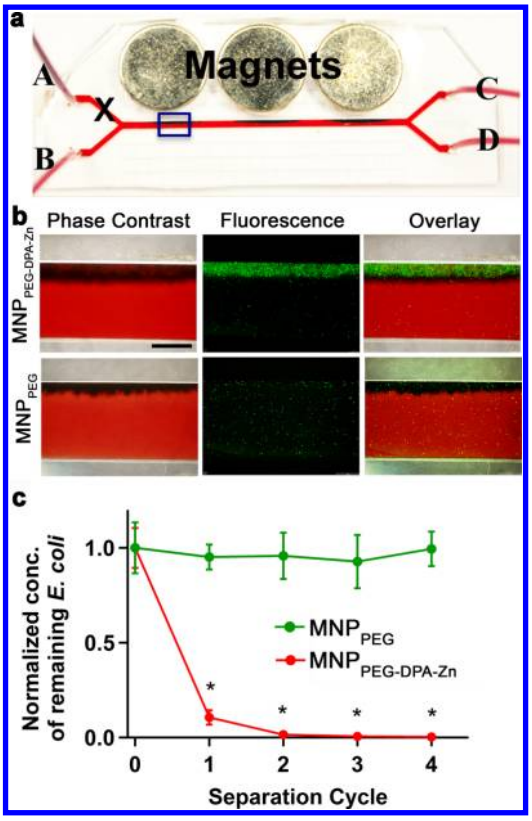

Figure 5. Magnetophoric separation of bacteria from whole blood. (a) Inlet A was closed. Three permanent magnet discs were placed along the main channel. Whole blood containing MNPs and fluorescently labeled *E. coli* was infused through inlet B and exited through outlets C and D. (b) Phase contrast and fluorescence micrographs of the area indicated by a box in panel a, and their overlay. $\mathbf{MNP_{PEG\text{-}DPA\text{-}Zn}}$ (dark in phase contrast) co-localized with *E. coli* (green fluorescence), while $\mathbf{MNP_{PEG}}$ accumulated without *E. coli*. (c) Effect of repeated cycles of separation on the concentration in whole blood of *E. coli* at outlet C normalized to the initial *E. coli* concentration. After each round of microfluidic separation, the solution collected at outlet D was reinfused at inlet B. Within two cycles of separation, all *E. coli* were removed from whole blood. Data are medians with 25th and 75th percentiles. ($N = 4$) $^*p < 0.01$ compared to the initial concentration.

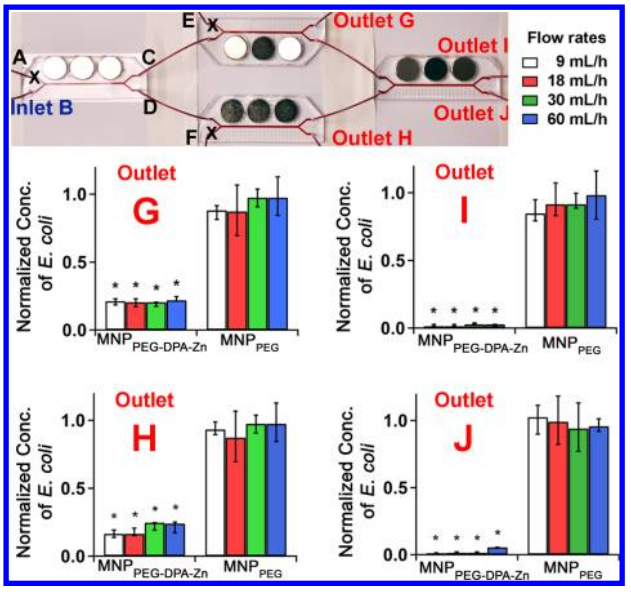

Figure 6. Normalized concentration of *E. coli* after sequential microfluidic separations using $\mathbf{MNP_{PEG\text{-}DPA\text{-}Zn}}$ in whole blood. Channels A, E, and F were closed. Blood was infused through inlet B and collected from outlets G, H, I, and J. *E. coli* concentrations were measured at various flow rates (9, 18, 30, and 60 mL/h). Data are medians with 25th and 75th percentiles ($N > 5$) of the concentrations of *E. coli* at the outlets normalized to the initial *E. coli* concentration (5.0×10^6 CFU/mL). There were no statistically significant differences among the four flow rates in all samples. $^*p < 0.05$ compared to the initial *E. coli* concentration.

10^6 CFU/mL) and MNPs (1.0×10^{11}/mL) was infused through the circuit, collected at outlet D and reinfused; this process was repeated for four cycles (Figure 5c). 88% of *E. coli* were removed during the first cycle of separation and complete removal of *E. coli* was achieved after the second cycle, whereas $\mathbf{MNP_{PEG}}$ did not affect the number of *E. coli*.

The performance of the microfluidic system was enhanced by connecting multiple devices in series and in parallel (Figure 6) so that multiple magnetic separations could be completed in a single pass. Inlets A, E, and F were closed so that B was the single inlet, through which the mixture of *E. coli* (5.0×10^6 CFU/mL) and MNPs (1.0×10^{11}/mL) in whole blood entered the system. The blood exiting outlets G and H had passed through two sites where magnetic separation took place, and those exiting I and J had passed through three. The concentration of *E. coli* at these outlets after magnetic separation is summarized in Figure 6. The concentration of *E. coli* in flows out of G and H was about 20% of the starting concentration, and much lower concentrations (<5%) were found in flows out of I and J. These significant reductions in bacterial concentrations were reproduced at all outlets at flow rates as high as 60 mL/h. This flow rate was much higher than those used in previously reported methods (e.g., 25 μL/h, 6.0 mL/h, and 20 mL/h).[16,17,26] There was no statistically significant difference between concentrations at G and H, or between I and J. When $\mathbf{MNP_{PEG}}$ was used, *E. coli* concentrations remained largely the same as the initial concentration.

With the MNP concentration (1.0×10^{11}/mL) used here, the accumulation of MNPs near the magnets limited the blood volume that could be filtered to approximately 2 mL per cycle. MNP buildup gradually reduced the efficiency of the magnetic separation. Employing stronger magnets, using an automated flushing system to remove the MNPs and/or increasing the contact areas between the magnets and the channels could mitigate these problems. It may also be possible to use lower concentrations of MNPs and/or to dilute the blood prior to processing.

In conclusion, we have developed a highly efficient method of removing both Gram-negative bacteria and endotoxins from blood. This method separated bacteria from blood with substantially shorter incubation times and at higher flow rates than have previously been reported, both of which are important parameters for clinical implementation as they affect the overall time that blood needs to be maintained outside the body without coagulating, becoming infected, etc. Although only *E. coli* was tested for magnetic separation, this approach could be broadly applicable among Gram-negative bacteria, which share common cell membrane structures. Devices of this kind could be adapted for clinical use in a manner analogous to equipment used for hemodialysis, hemofiltration, plasmapheresis, and extracorporeal membrane oxygenation to remove pathogens in acute situations.

dx.doi.org/10.1021/nl3047305 | *Nano Lett.* XXXX, XXX, XXX−XXX

■ ASSOCIATED CONTENT

Supporting Information

Experimental details, characterization of materials, hemolysis and demonstration of a two-inlet microfluidic system (both figures and movies). This material is available free of charge via the Internet at http://pubs.acs.org.

■ AUTHOR INFORMATION

Corresponding Author

*E-mail: Daniel.Kohane@childrens.harvard.edu. Telephone: 617-919-2364. Fax: 617-730-0453.

Author Contributions

‡Contributed equally

Notes

The authors declare no competing financial interest.

■ ACKNOWLEDGMENTS

This work was supported by Dr. Kohane's Biotechnology Research Endowment through the Department of Anesthesiology at Boston Children's Hospital.

■ REFERENCES

(1) Cohen, J. *Nature* **2002**, *420* (6917), 885−891.
(2) Angus, D. C.; Linde-Zwirble, W. T.; Lidicker, J.; Clermont, G.; Carcillo, J.; Pinsky, M. R. *Crit. Care Med.* **2001**, *29* (7), 1303−1310.
(3) Murphy, S. L.; Xu, J.; Kochanek, K. D. *Natl. Vital Stat. Rep.* **2012**, *60*, 1−52.
(4) Hotchkiss, R. S.; Karl, I. E. *New Engl. J. Med.* **2003**, *348* (2), 138−150.
(5) Venkataraman, R.; Subramanian, S.; Kellum, J. A. *Crit. Care* **2003**, *7* (2), 139−145.
(6) Annane, D.; Bellissant, E.; Bollaert, P. E.; Briegel, J.; Keh, D.; Kupfer, Y. *Brit. Med. J.* **2004**, *329* (7464), 480−484.
(7) Levi, M.; De Jonge, E.; Van Der Poll, T. *Int. J. Clin. Pract.* **2002**, *56* (7), 542−545.
(8) Garnacho-Montero, J.; Aldabo-Pallas, T.; Garnacho-Montero, C.; Cayuela, A.; Jimenez, R.; Barroso, S.; Ortiz-Leyba, C. *Crit. Care* **2006**, *10*, 4.
(9) Bouman, C. S. C.; Straaten, H. M. O.-v.; Schultz, M. J.; Vroom, M. B. *J. Crit. Care* **2007**, *22* (1), 1−12.
(10) Neu, H. C. *Science* **1992**, *257* (5073), 1064−1073.
(11) Valles, J.; Rello, J.; Ochagavia, A.; Garnacho, J.; Alcala, M. A. *Chest* **2003**, *123* (5), 1615−1624.
(12) Harbarth, S.; Garbino, J.; Pugin, J.; Romand, J. A.; Lew, D.; Pittet, D. *Am. J. Med.* **2003**, *115* (7), 529−535.
(13) Hoffmann, J. N.; Hartl, W. H.; Deppisch, R.; Faist, E.; Jochum, M.; Inthorn, D. *Kidney Int.* **1995**, *48* (5), 1563−1570.
(14) Gardlund, B. *Acta Anaesth. Scand.* **2006**, *50* (8), 907−910.
(15) Eichacker, P. Q.; Natanson, C.; Danner, R. L. *New Engl. J. Med.* **2006**, *355* (16), 1640−1642.
(16) Qiu, J.; Zhou, Y.; Chen, H.; Lin, J.-M. *Talanta* **2009**, *79* (3), 787−795.
(17) Xia, N.; Hunt, T. P.; Mayers, B. T.; Alsberg, E.; Whitesides, G. M.; Westervelt, R. M.; Ingber, D. E. *Biomed. Microdevices* **2006**, *8* (4), 299−308.
(18) O'Neil, E. J.; Smith, B. D. *Coordin. Chem. Rev.* **2006**, *250* (23−24), 3068−3080.
(19) Lakshmi, C.; Hanshaw, R. G.; Smith, B. D. *Tetrahedron* **2004**, *60* (49), 11307−11315.
(20) Ngo, H. T.; Liu, X.; Jolliffe, K. A. *Chem. Soc. Rev.* **2012**, *41* (14), 4928−4965.
(21) Leevy, W. M.; Gammon, S. T.; Jiang, H.; Johnson, J. R.; Maxwell, D. J.; Jackson, E. N.; Marquez, M.; Piwnica-Worms, D.; Smith, B. D. *J. Am. Chem. Soc.* **2006**, *128* (51), 16476−16477.
(22) Leevy, W. M.; Gammon, S. T.; Johnson, J. R.; Lampkins, A. J.; Jiang, H.; Marquez, M.; Piwnica-Worms, D.; Suckow, M. A.; Smith, B. D. *Bioconjugate Chem.* **2008**, *19* (3), 686−692.
(23) Leevy, W. M.; Johnson, J. R.; Lakshmi, C.; Morris, J.; Marquez, M.; Smith, B. D. *Chem. Commun.* **2006**, *15*, 1595−1597.
(24) White, A. G.; Gray, B. D.; Pak, K. Y.; Smith, B. D. *Bioorg. Med. Chem. Lett.* **2012**, *22* (8), 2833−2836.
(25) Thakur, M. L.; Zhang, K.; Paudyal, B.; Devakumar, D.; Covarrubias, M. Y.; Cheng, C.; Gray, B. D.; Wickstrom, E.; Pak, K. Y. *Mol. Imaging. Biol.* **2012**, *14* (2), 163−171.
(26) Yung, C. W.; Fiering, J.; Mueller, A. J.; Ingber, D. E. *Lab Chip* **2009**, *9* (9), 1171−1177.
(27) Tajima, N.; Takai, M.; Ishihara, K. *Anal. Chem.* **2011**, *83* (6), 1969−1976.
(28) Burry, R. W. Antibodies. *Immunocytochemistry: a Practical Guide for Biomedical Research*, Springer: New York, 2010, pp 7−16.
(29) Chapman, A. P. *Adv. Drug Deliver. Rev.* **2002**, *54* (4), 531−545.
(30) Kohane, D. S. *Biotechnol. Bioeng.* **2007**, *96* (2), 203−209.
(31) Jia, H. F.; Zhu, G. Y.; Wang, P. *Biotechnol. Bioeng.* **2003**, *84* (4), 406−414.
(32) Pamme, N. *Lab Chip* **2007**, *7* (12), 1644−1659.
(33) Lenshof, A.; Laurell, T. *Chem. Soc. Rev.* **2010**, *39* (3), 1203−1217.
(34) Wu, Z.; Willing, B.; Bjerketorp, J.; Jansson, J. K.; Hjort, K. *Lab Chip* **2009**, *9* (9), 1193−1199.
(35) Mach, A. J.; Di Carlo, D. *Biotechnol. Bioeng.* **2010**, *107* (2), 302−311.
(36) Helton, K. L.; Yager, P. *Lab Chip* **2007**, *7* (11), 1581−1588.
(37) Sia, S. K.; Whitesides, G. M. *Electrophoresis* **2003**, *24* (21), 3563−3576.
(38) Wei Hou, H.; Gan, H. Y.; Bhagat, A. A. S.; Li, L. D.; Lim, C. T.; Han, J. *Biomicrofluidics* **2012**, *6* (2), 24115−2411513.
(39) El-Boubbou, K.; Gruden, C.; Huang, X. *J. Am. Chem. Soc.* **2007**, *129* (44), 13392−13393.
(40) Shih, P.-H.; Shiu, J.-Y.; Lin, P.-C.; Lin, C.-C.; Veres, T.; Chen, P. *J. App. Phys.* **2008**, *103*, 07A316.
(41) Taylor, F. B. *Crit. Care Med.* **2001**, *29* (7), S78−S89.
(42) Boulos, L.; Prevost, M.; Barbeau, B.; Coallier, J.; Desjardins, R. *J. Microbiol. Methods* **1999**, *37* (1), 77−86.
(43) Kepner, R. L.; Pratt, J. R. *Microbiol. Rev.* **1994**, *58* (4), 603−615.
(44) Demidova, T. N.; Gad, F.; Zahra, T.; Francis, K. P.; Hamblin, M. R. *J. Photochem. Photobiol. B* **2005**, *81* (1), 15−25.
(45) Hurley, J. C. *Clin. Microbiol. Rev.* **1995**, *8* (2), 268−292.